

Microwave response of a Josephson junction in YBCO on a substrate with a low step

K. I. Konstantinyan, A. D. Mashtakov* G. A. Ovsyannikov J. Ramos,[†] and Z. G. Ivanov[†]

Institute of Radio Engineering and Electronics, Russian Academy of Sciences, 103907 Moscow, Russia

(Submitted 30 January 1995)

Zh. Éksp. Teor. Fiz. **107**, 1742–1755 (May 1995)

The processes associated with the interaction of an electromagnetic field with single and double high- T_c superconducting ($\text{YB}_2\text{C}_3\text{O}_x$) bicrystal boundaries obtained as a result of the oblique ion milling of steps on MgO substrates have been investigated experimentally for various values of the temperature from $T \approx 4.2$ –77 K, the magnetic field from $B \approx -0.4$ – $+0.4$ mT, and the power of microwave radiation with a frequency $f_e \approx 30$ –52 GHz. The results obtained and the data from numerical simulation have confirmed a hypothesis that current is transported through the bicrystal boundaries by individual isolated regions that can be modeled by Josephson junctions, each of which is described by the known resistively shunted junction (RSJ) model. The physical mechanisms causing the behavior of the bicrystal boundaries to deviate from the RSJ model, particularly the observed upward deviation (in comparison to theory) of the range of currents for frequency (both harmonic and subharmonic) synchronization of the spontaneous Josephson emission by an external microwave field, have been discussed. © 1995 American Institute of Physics.

1. INTRODUCTION

The high anisotropy and short coherence length (of the order of an interatomic distance) of high- T_c metal-oxide superconductors impose considerable restrictions on the creation of Josephson junctions for known reasons (see, for example, Ref. 1). There has recently been widespread interest in some unconventional types of Josephson junctions, which utilize the experimentally established formation of weak links on the boundaries of the crystalline grains in epitaxial films deposited on a substrate with a specially created imperfection: a bicrystal boundary, a step on the substrate surface, etc.^{2–11} The substrate imperfection serves as a seed for the formation of a grain boundary having the properties of a Josephson junction in an epitaxial high- T_c superconducting film. For junctions formed on a substrate with a step, the cases in which either one or two grain boundaries operate in the working range of currents should be distinguished. The existence of an array of two grain boundaries has been observed repeatedly in experiments,⁵ but the case of a single grain boundary is predominant and has been investigated to a relatively great extent,^{6,7,10–13} while there are practically no data on investigations of junctions with a double grain boundary. This is attributed to the fact that grain boundaries form at the sites of breaks in the substrate surface on a step with a height h similar to or somewhat greater than the thickness d of the high- T_c superconducting film.³ In this case the tilt angle of the epitaxial film on the step edge relative to the plane of the substrate is greater than 60° , and the conditions for formation of the upper and lower grain boundaries differ significantly.¹³

The modification of step-edge junctions by decreasing the step height (to a value less than the thickness of the high- T_c superconducting film) and employing oblique ion milling of the substrate was recently proposed.^{8,10} One special feature of the junctions obtained by this method is the fact that a portion of the epitaxial $\text{YB}_2\text{C}_3\text{O}_x$ (YBCO) film

which is rotated 45° in the ab plane and has two in-plane bicrystal boundaries at the seams with the main film forms in the vicinity of the step on the substrate. Both the case of a single bicrystal boundary, in which the difference between the critical currents of the two bicrystal boundaries is large, i.e., $I_{c1} \ll I_{c2}$, and the case of two bicrystal boundaries with similar values, i.e., $I_{c1} \approx I_{c2}$, are observed here experimentally, just as in the case of junctions on a high step. Recent investigations of a Josephson junction on a single grain boundary demonstrated that relatively satisfactory correspondence to the resistively shunted junction (RSJ) model of a Josephson junction having a current-voltage characteristic of hyperbolic form and known¹ behavior of the Josephson current steps under the action of an external microwave signal is achieved either at temperatures near the critical temperature¹² or when certain conditions are imposed on the geometry of the junction and the strength of the applied constant magnetic field.¹⁰ The first measurements of the parameters of Josephson emission from grain boundaries also attested to considerable deviations of their behavior from the RSJ model,^{7,12,13} which were manifested by significant broadening of the emission line and a deviation from the Lorentzian line shape. At the same time, detailed investigations of the low-frequency noise and magnetic measurements indicated that a high- T_c superconducting junction should be regarded as a complicated multielement Josephson structure, which can be modeled in some cases by a one-dimensional array of N Josephson junctions which are connected in parallel and have a small dimension $w < \lambda_j$ (w is the dimension of the film forming the Josephson junction perpendicular to the direction of flow of the transport current I , and λ_j is the Josephson penetration depth of a magnetic field into the weak-link region). A comparison of the experiment with the results of the numerical simulations in Refs. 10 and 11 confirmed the validity of such a model, which explains, in particular, the formation of subharmonic current steps.

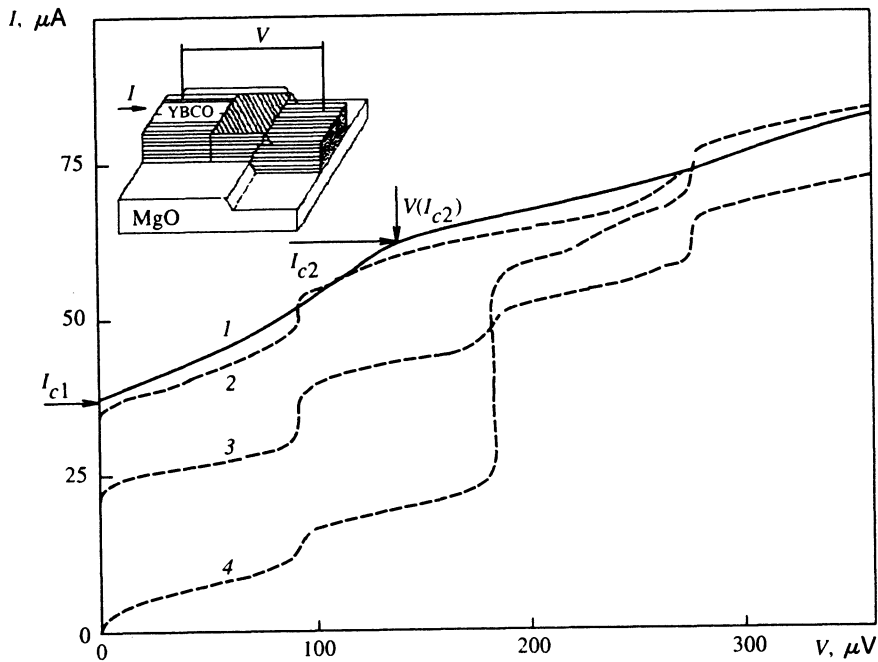


FIG. 1. Unperturbed current-voltage characteristic of Josephson structure YA2.6J2 (solid line 1) and its current-voltage characteristics under external microwave radiation with a frequency of 45 GHz at $T=4.2$ and various relative levels of attenuation of the microwave power: 2) 20 dB; 3) 10 dB; 4) 5 dB. The arrows mark the critical currents of the first and second bicrystal boundary, respectively. A substrate with a high- T_c bridge structure is schematically represented in the insert. The hatched region to the left of the step corresponds to a film which is turned 45° in the ab plane and forms two bicrystal boundaries connected in series. The arrow shows the direction of the transport current. The external magnetic field was perpendicular to the plane of the substrate.

In this report we present the results of experimental investigations and the dynamic high-frequency characteristics of YBCO Josephson structures on substrates with a low step, both with a single bicrystal boundary and with a double bicrystal boundary, at various values of the temperature T in a weak external magnetic field B .

2. EXPERIMENTAL METHOD

Low steps ($h=2-5$ nm) were formed on an MgO substrate using a photoresist mask by ion milling at a 60° angle to the plane of the substrate. After the resist was stripped, a YBCO film with a thickness $d=250$ nm was laser-deposited at $600-700^\circ\text{C}$. The YBCO films obtained were oriented parallel to the c axis and had a critical temperature $T_c=89-91$ K. A thin-film bridge with a width $w=4-8$ μm was formed across each step by photolithography followed by ion milling of the YBCO film.⁸ The high critical current density $j_c=I_c/wd>10^7$ A/cm² ($T=4.2$ K) of the YBCO film measured on both sides of the step attests to its uniformity and the absence of weak links in it. The value of j_c for the bridge spanning the step decreased to 10^2-10^5 A/cm², attesting to the formation of a weak link in the thin film.

The unperturbed current-voltage characteristics of the Josephson structures, as well as the current-voltage characteristics recorded under electromagnetic radiation in the millimeter range (with a frequency of 30–50 GHz) and a constant external magnetic field, were investigated. The measurements were performed in a shielded room with thorough filtering of the signals from the electric lines entering the cryostat. Partial synchronization of the spontaneous emission by a weak external electromagnetic field results in the appearance of a detector response η (Ref. 14) with an odd-resonant form in the range of voltages on the Josephson junction $V \approx hf_e/2e$, where f_e is the frequency of the external field. A plot of $\eta(V)$ can serve as a convenient test for comparing the dynamic characteristics of an unperturbed Jo-

sephson structure (the width of the Josephson emission line, the frequency spectrum of the spontaneous emission, etc.) with theoretical models. The response of each Josephson structure to the high-frequency electromagnetic field and the constant magnetic fields was numerically simulated using the PSCAN program,¹⁵ which makes it possible to automatically formulate the system of differential equations describing a circuit containing several Josephson junctions and integrate it with respect to time with a variable spacing.

3. EXPERIMENTAL RESULTS AND DISCUSSION

The investigations of the region of a Josephson structure under a transmitting electron microscope revealed that the YBCO film contains two bicrystal boundaries formed by 45° rotation of the bridge film fragment near the step in the ab plane.⁸ A substrate with a step and a thin YBCO film deposited on it is schematically represented in the insert in Fig. 1. The orientations of the YBCO film and the MgO substrate in the ab plane coincided on both the milled side and the side protected from milling, while in the immediate vicinity of the step, the YBCO film was turned 45° . The position of the portion of the film rotated in the ab plane (the oblique hatching to the left of the step) shows that growth of this film occurs in the region shielded by the photoresist mask during ion milling.

The typical current-voltage characteristic shown in Fig. 1 has two sections with an almost constant differential resistance R_d separated by a feature with an abrupt increase in R_d . This form of the current-voltage characteristic is caused by the fact that due to the difference between the critical currents $I_{c1} < I_{c2}$ of the two bicrystal boundaries, successive passage of the boundaries into the resistive state is observed as the transport current is increased, the section with the sharp change in R_d corresponding to the larger critical current I_{c2} . The application of microwave radiation in the millimeter range confirms that there are two bicrystal bound-

TABLE I. Parameters of the samples investigated.

Sample	h , nm	w , μm	R_N , Ω	$I_{c1}(T = 4, 2 \text{ K})$, μA	$V(I_{c2})$, μV
YA2.6J1	3	8	1	100	> 1000
YA2.6J2	3	4	6	36	140
YA2.4J1	3	8	36	30	120
YA2.3J5	5	8	2	7500	> 1000
YA2.7J5	2	8	2	3000	> 1000
YA2.24J3	10	7	2	80	70

aries connected in series. When the power P_e of the microwave radiation is at a low level (curve 2 in Fig. 1), the current-voltage characteristic displays two Josephson current steps, one on each side of $V(I_{c2})$. The current step at small $V < V(I_{c2})$ is related exactly to the frequency of the incident radiation f_e by the Josephson relation: $V = V_{n,m} = nmhf_e/2e$ when $n = m = 1$, where n is the number of the harmonic of the external microwave field causing synchronization of the Josephson emission and m is the number of Josephson junctions connected in series that participate in the synchronization process. The second step in the current-voltage characteristic at $V_{1,2} > V(I_{c2})$ is sloped, and its position depends on P_e due to the summation of the resistive contribution of the first bicrystal boundary and the current step on the second bicrystal boundary. When the power P_e is increased, the current steps on the two bicrystal boundaries can overlap, but the numbers n corresponding to them need not coincide. As a result, mutually parallel vertical current steps form in the current-voltage characteristic at values of $V_{n,2}$ where the emission frequencies of the two bicrystal boundaries are multiples of $2eV/h$, while the phase difference of the emissions can take any value (Fig. 1, curves 3 and 4). This regime differs from the case of phase locking in an array of connected Josephson junctions, in which the phase difference of the Josephson emissions is dictated by the external electrodynamic coupling of the Josephson junctions.¹⁶

The dynamic characteristics of similar structures with two Josephson junctions connected in series are determined primarily by the difference between the critical currents of the bicrystal boundaries. However, when the dynamics of the processes in Josephson junctions are investigated in the vicinity of the first harmonic f of the spontaneous Josephson emission or in the presence of microwave radiation with a frequency $f_e \approx f$, the relationship between the voltages in the Josephson structure is significant. For example, when the difference between the parameters is small, f_e is high, and thus $V(I_{c2}) < V_{1,1}$, the response of the Josephson structure is determined by the interaction of the two bicrystal boundaries and the synchronization of their oscillations by the external force. When $V(I_{c2}) \gg V_{1,1}$ and thus $I_{c1} \ll I_{c2}$, the influence of the Josephson junction with the larger critical current can be neglected in a first approximation, if it is assumed that the dynamics of the processes in a Josephson structure are determined by only one bicrystal boundary, while the other bicrystal boundary is in the superconducting state. The results of measurements of several samples at $T = 4.2 \text{ K}$ are presented in Table I. We shall begin a more detailed discussion of the Josephson structures with the first case.

3.1. Two bicrystal boundaries in series

The current-voltage characteristics of Josephson structure YA2.24J3, which satisfies the condition $V(I_{c2}) \leq V_{1,1}$, were measured for three fixed frequencies $f_e = 36, 44$, and 52 GHz at $T = 4.2 \text{ K}$, at which the influence of thermal noise can be neglected. We note that the case of $f_e = 36 \text{ GHz}$ corresponds to the condition $V(I_{c2}) = V_{1,1}$. Figure 2 presents a set of current-voltage characteristics for various levels of external electromagnetic power with $f_e = 52 \text{ GHz}$. We determined the critical current I_{c2} and the amplitude of the current step I_{12} of the second bicrystal boundary from the features in the current-voltage characteristics marked with arrows in Fig. 2. It is seen from the figure that the current step at $V = V_{1,2}$, which corresponds to summation of the $n = 1$ steps of two bicrystal boundaries, is most clearly displayed. The presence

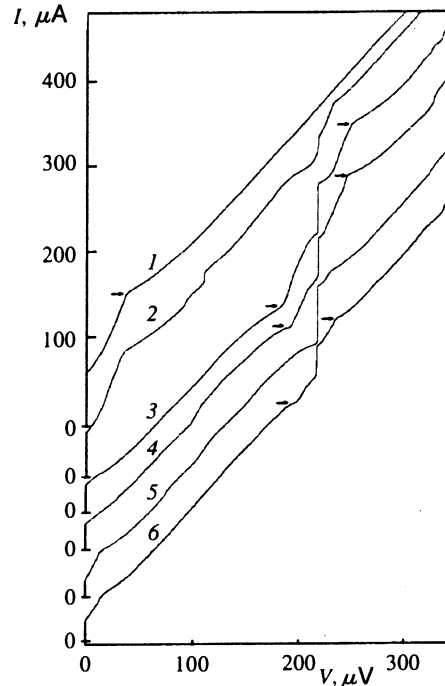


FIG. 2. Unperturbed current-voltage characteristic of Josephson structure YA2.24J3 (1) and its current-voltage characteristics under external microwave radiation with a frequency of 52 GHz at $T = 4.2$ and various relative microwave power levels, dB: 2) 32.5; 3) 21; 4) 17.4; 5) 15.2; 6) 12.8. The arrows point out features corresponding to the transition to the resistive state and the appearance of the current step of the second junction. Curves 2–6 have been displaced along the current axis for clarity, but the scale for I is the same as for curve 1.

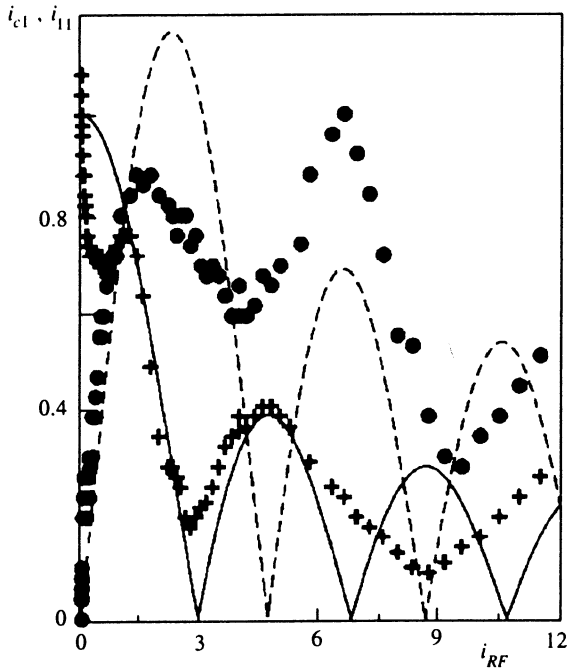


FIG. 3. Dependence of the normalized values of the critical current $i_{c1} = I_{c1}/I_{c1}(0)$ (crosses—experiment; solid line—theory) and the current step $i_{11} = I_{11}/I_{c1}(0)$ (filled circles—experiment; dashed line—theory) on the amplitude of the current of the microwave radiation i_{RF} for a voltage $V_{1,2}$ on the bicrystal boundaries at $T = 4.2$ K and $f_e = 52$ GHz.

of two bicrystal boundaries is also indicated by the features of the current-voltage characteristic in the vicinity of the step at $V = V_{1,2}$ (see, for example, curves 3 and 4 in Fig. 2). Here the vertical step corresponds to the summation of the steps of two bicrystal boundaries synchronized by the external field, and the features in the current-voltage characteristic in the form of a change in R_d are caused by the presence of a step on only one of the bicrystal boundaries. It should be noted that vertical current steps were also observed at $V = V_{2,2}$ (beyond the range of voltages shown in the figure) for all other values of f_e . Curve 2 also shows a vertical subharmonic step with $n = 1/2$ and $m = 2$. We note that over the entire range of voltages investigated $V \leq 0.5$ mV, the subharmonic current steps detected at $V_{n,2}$ were multiples of $n = 1/4$ and periodically transformed from sloped to parallel steps and back due to the more severe conditions for their locking by the external force.

The values of the critical currents and the amplitudes of the Josephson current steps, including the subharmonic steps, exhibited an oscillatory dependence on the normalized amplitude of the external field $i_{RF} = I_{RF}/I_c(0)$ for both bicrystal boundaries. Figure 3 presents experimental plots of the dependence of the normalized values of the critical current $i_{c1} = I_{c1}/I_{c1}(0)$ and of the amplitude of the current step $i_{11} = I_{11}/I_{c1}(0)$ at $V = V_{1,2}$ on i_{RF} , which were obtained from a treatment of the experimental current-voltage characteristics for $f_e = 52$ GHz. The theoretical plots for the critical current and the first current step presented in Fig. 3 were obtained from the RSJ model for a single Josephson junction with consideration of the experimental value of

$hf_e/2eI_{c1}R_{N1} \approx 1.65$, where R_{N1} is the normal-state resistance of the first bicrystal boundary determined from the value of R_d at $V < V(I_{c2})$.

It can be seen from Fig. 3 that the plots of i_{c1} and i_{11} in the range $i_{RF} < 4.5$ [up to the first minimum of the function $i_{c1}(i_{RF})$] exhibit relatively satisfactory agreement with the theoretical plots. This is evidence that the estimated critical frequency f_c of the Josephson structure determined from dc measurements according to the formula $f_c = (2e/h)V_0$ ($V_0 = I_c R_N$, where R_N is the value of the normal-state resistance of the Josephson junction), is close to the value of f_c dictating the dynamics of the Josephson structure.¹ At relatively high values of $i_{RF} > 5$ there is a significant difference between the experimental values of i_{11} and the theoretical value. For example, the second and third local maxima of $i_{11}(i_{RF})$ significantly exceed the theoretical value. It should be noted that in the case of two independent Josephson junctions connected in series, such an upward deviation [$i_{11}(i_{RF} \approx 6) \approx 1$] is impossible according to the RSJ model.¹⁶ A similar upward deviation of the maximum amplitude of the Josephson current step at $V = V_{1,2}$ was previously observed for a closely arranged pair of tin microbridges of variable thickness and was caused by their interaction by means of nonequilibrium quasiparticles.^{16,17} At the same time, the detector response of the Josephson structure with two bicrystal boundaries to a weak signal $i_{RF} \leq 0.1$ with $f_e \approx f$ did not have the odd-resonant form characteristic of phase-dependent selective detection.¹ Variation of the magnetic field, even in the case in which the critical currents of the bicrystal boundaries were equal, i.e., $I_{c1} = I_{c2}$ (sample YA2.6J2), did not produce a synchronous detector response. This attests to passage from a regime with the mutually independent spontaneous Josephson emission of two bicrystal boundaries to a partially coherent regime under the action of the external electromagnetic field,¹⁸ which is most likely due to the small but finite coupling energy of the bicrystal boundaries, as well as the influence of the load impedance of the microwave waveguide loop shunting the Josephson structure.

3.2. Single bicrystal boundary

In the case of Josephson structures for which $I_{c1} \ll I_{c2}$ (see Fig. 4), the unperturbed current-voltage characteristic had only one section with an increase in R_d at small values of $V < V_0$ with a form similar to the RSJ model. At the same time, some differences from the RSJ model were observed. For example, at $I \gg I_c$ (as for a Josephson structure with two bicrystal boundaries) there was an appreciable excess current (a shift in the current-voltage characteristic relative to the plot of $V = IR_N$), which is characteristic of weak links with a nontunneling type of conduction. It is seen that under the microwave radiation, current steps appear in the current-voltage characteristics at $V = V_{n,1}$ (dashed curves in Fig. 4). Here the subharmonic steps with $n = 1/2$ and $3/2$ (see curve 3) had an oscillatory dependence on i_{RF} (see the insert in Fig. 4), were mutually parallel, first appeared at small values of $i_{RF} > 0.2$, and increased in size with increasing i_{RF} along the sequence $n = 1/2, 1, 3/2, 2$, etc. We note that subharmonic current steps are not observed for a single Josephson junction according to the RSJ model.¹ Regardless of their number, the

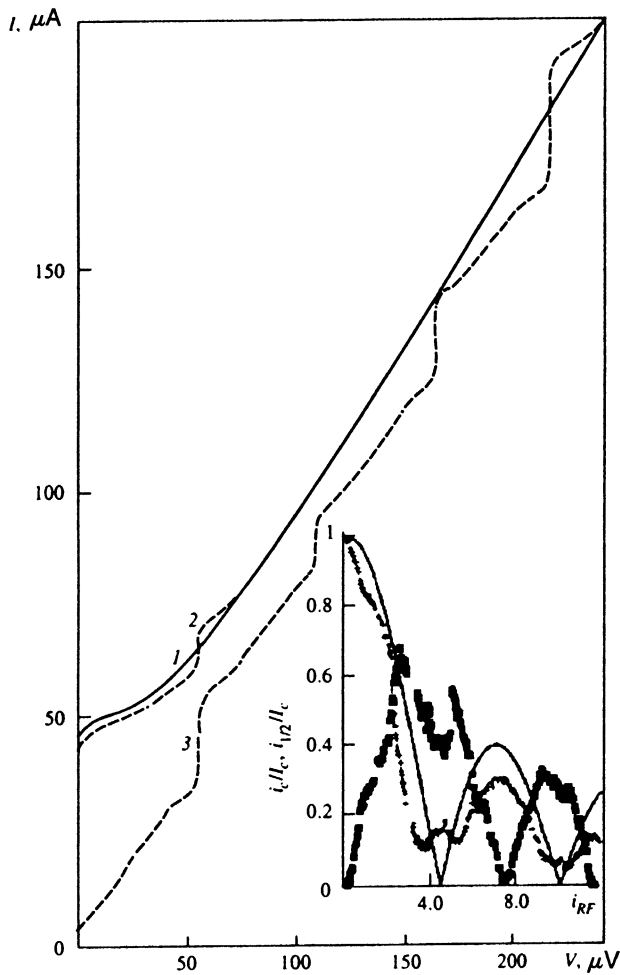


FIG. 4. Unperturbed current-voltage characteristic of Josephson structure YA2.6J1 with one "working" bicrystal boundary (1) and its current-voltage characteristic under external microwave radiation with a frequency of 52 GHz at $T=4.2$ K at different levels of the microwave power: 2) 26 dB; 3) 5.6 dB. The insert contains normalized plots of the dependence of the critical current (crosses) and the $n=1/2$ subharmonic current step (squares) on the microwave current. The solid line is a theoretical plot of $i_c(i_{RF})$ according to the RSJ model.

current steps in the experimental perturbed current-voltage characteristics intersected the unperturbed characteristic at definite values of $i_{RF} \leq 2$ and had a nearly hyperbolic form. The insert in Fig. 4 shows plots of the dependence of the critical current $i_c = I_c/I_c(0)$ and the subharmonic step $i_{1/2} = I_{1/2}/I_c(0)$ on i_{RF} obtained for a frequency of 52 GHz at $T=4.2$ K, and the solid line is a theoretical plot of $i_c(i_{RF})$ based on the RSJ model for the experimental value of $hf_e/2eV_0 \approx 1.5$. It is seen that the oscillation period of the experimental plot of $i_c(i_{RF})$ corresponds to the RSJ model, although the positions of the minima of $i_c(i_{RF})$ are broadened significantly. It is also seen that the values of i_{RF} at the features (dips) in the plot of $i_{1/2}(i_{RF})$ in the regions of the maxima correspond to the values of i_{RF} at the features (humps) in the plot of $i_c(i_{RF})$ in the vicinity of the minima.

Better agreement between experiment and the RSJ model was observed for some samples when the temperature was increased. For example, at $T=77$ K the oscillation period of $i_c(i_{RF})$ and the height of the first maximum corre-

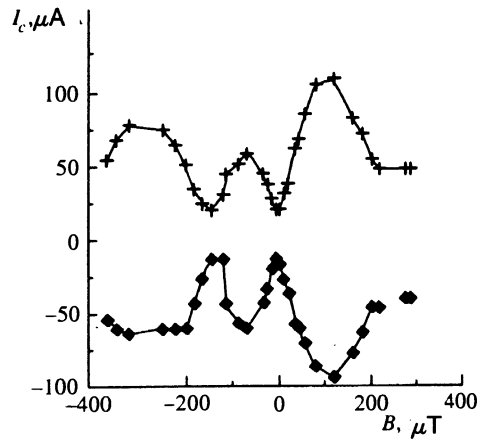


FIG. 5. Dependence of the critical current on the magnetic induction for the forward (crosses) and reverse (squares) directions of the transport current for Josephson structure YA2.6J1 at $T=4.2$ K.

sponded to the RSJ model of a Josephson junction to significantly greater (10%) accuracy, and subharmonic current steps were no longer detected.

Figure 5 shows the experimental dependence of the critical current on the external magnetic field perpendicular to the plane of a substrate with a Josephson structure at $T=4.2$ K. It can be seen that regardless of the direction of the transport current, the form of the periodic function $I_c(B)$ is nearly symmetric about $I=0$. The minimum of $I_c(B)$ at $B=0$ is most likely due to the lack of cancellation of the residual field B_a near the value of the earth's field. A significant difference between the plots obtained and the "Fraunhofer" dependence typical of a Josephson junction with a uniform distribution of the critical current density is observed. The experimental plot of $I_c(B)$ is closer in form to two Josephson junctions (SQUIDS) connected in parallel than to a single Josephson junction. Moreover, the appearance of higher maxima as B increases attests to a significantly nonuniform distribution of the current density on the bicrystal boundary.^{4,11} The similarity of $I_c(B)$ to plots for SQUIDS was maintained at higher temperatures ($T > 4.2$ K). Such behavior of the Josephson structure was most likely caused by the significant nonuniformity of the bicrystal boundary, which has also been observed for some other junctions on grain boundaries.³ The simplest model of such junctions may be an array of lumped Josephson junctions connected in parallel, but separated by the inductances of the superconducting edges.¹¹

4. NUMERICAL SIMULATION AND COMPARISON WITH EXPERIMENT

A single bicrystal boundary was numerically simulated using a model consisting of an array of N Josephson junctions of small dimensions connected in parallel by inductances (such an array of five Josephson junctions is shown in Fig. 6a). The number of Josephson junctions in the array was varied from $N=4 \dots 8$. The current was fed symmetrically to the ends of the array. This corresponded to an experiment in which the constant current in the Josephson structure was

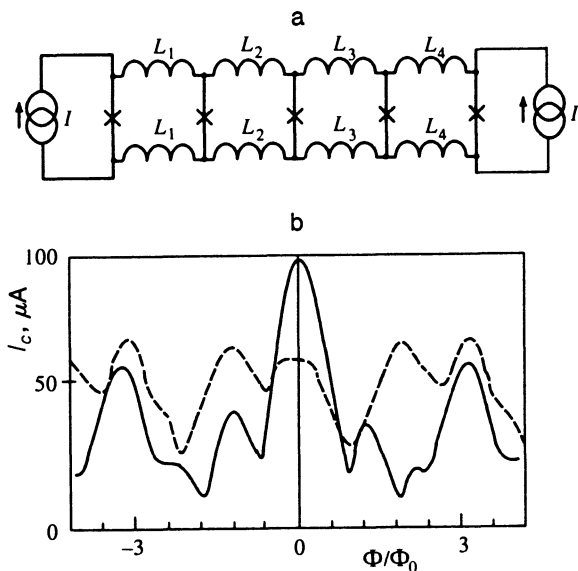


FIG. 6. (a) Model of an array of $N=5$ Josephson junctions connected in parallel by the inductances $L_1 \dots L_{N-1}$. (b) Dependence of the critical current I_c on the magnetic flux calculated for model (a): dashed line—calculation for the case of large inductances ($L_1=L_2=13$ pH, $L_3=L_4=26$ pH) when spreading of the end currents occurs; solid curve—calculation for the case of small inductances ($L_1=L_2=1.3$ pH, $L_3=L_4=2.6$ pH).

supplied through a superconducting film. As we know, the constant current in a superconducting film of width w flows mainly along the edges in layers of width λ_{\perp} , where $\lambda_{\perp} = \lambda_L^2/d$ is the penetration depth of a magnetic field into a superconducting thin film of thickness $d < \lambda_L$ and λ_L is the London penetration depth of a magnetic field. To describe each of the Josephson junctions we used the RSJ model with a small capacitance (a McCumber parameter $\beta_C = 2\pi f_c CR_N \ll 1$, where C is the capacitance of the Josephson junction), in which the parameter $V_0 = 100 \mu\text{V}$ was fixed and the critical currents of all the Josephson junctions in the array were assigned identical values, which were chosen on the basis of the fixed value of the critical current of the entire array. In the calculations under discussion I_c was selected equal to $100 \mu\text{A}$, which corresponds to sample YA2.6J1 (see Table I). The inductances satisfied the condition $L_1 + L_2 + \dots + L_N = 8$ pH, which is equal to the inductance $L = \mu_0 w$ ($\mu_0 = 4\pi \cdot 10^{-7}$ H/m is the magnetic permeability of the vacuum) of a slot-shaped line with a length equal to the width of the bridge $w = 8 \mu\text{m}$. When the inductances were equal, the critical currents of the Josephson junctions in the array were approximately $20 \mu\text{A}$. The source electric current in the calculations was equal to the sum of the constant component and the oscillating addition, and we considered the time-averaged voltage on the Josephson junctions as the modeling output parameter. We note that with the inductance values selected, the total critical current of the array amounted to 97% of the sum of the critical currents of $N=5$ Josephson junctions, and the dimensionless inductance of the loops $l = (2\pi/\Phi_0)2LI_c$ (Φ_0 is the quantum of magnetic flux) was of order $l = 0.02-0.1$, depending on N .

It turned out that the model displays behavior qualitatively similar to the experimental results by $N=5$; therefore,

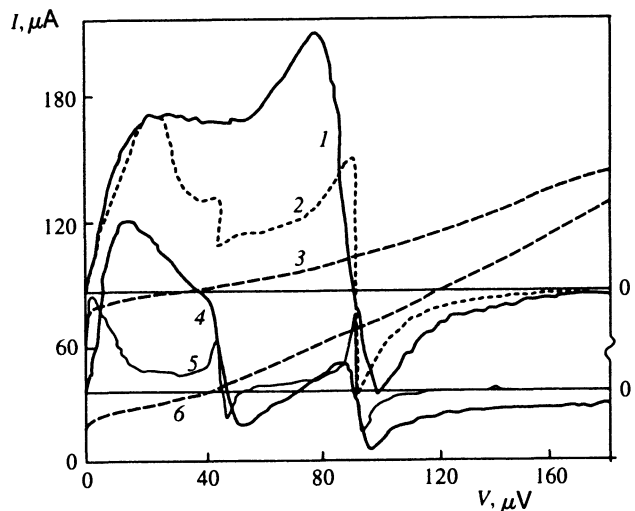


FIG. 7. Current-voltage characteristic (dashed line) of a Josephson structure at $T=4.2$ K and corresponding detector responses $\eta(V)$ to microwave radiation with a frequency $f_e=30.5$ GHz when $B=52 \mu\text{T}$ (curves 1, 2, and 3) and $B=-153 \mu\text{T}$ (curves 4, 5, and 6). The results of the numerical simulation of $\eta(V)$ obtained for fixed experimental values of $I_c(B)$ are represented by the dot-dashed and thin lines.

all the data from the calculations are presented for this case. Figure 6b presents the dependence of the critical current I_c of the array on the magnetic flux supplied to each of the four loops in the array. The values of the magnetic flux were proportional to the inductances forming the loops, so that the magnetic field was identical across all loops. The mean flux in all loops of the array is plotted on the horizontal axis in Fig. 6b. For small values of $L_1 + L_2 + L_3 + L_4 < 8$ pH the maximum value of I_c for the array is observed when $B=0$. The plot of $I_c(B)$ has local maxima with different heights, which are attributed to the interference of two oscillatory dependences of the critical current with two periods. The twofold difference between the periods was stipulated by the intentional selection of sets of values for the inductances of the superconducting loops in which $L_1/L_3 = L_2/L_4 = 2$.

A similar plot of $I_c(B)$ is also observed experimentally (see Fig. 5). The dashed line in Fig. 6b is a plot of $I_c(B)$ calculated for the case of large inductances. Here the maximum value of I_c is achieved as soon as $B \neq 0$. This result is attributed to spreading of the currents supplied to the ends of the array and is possible only with sufficiently large values of $l \approx 1$. In this case better agreement with experiment is observed, but the values selected for L_N ($N=1 \dots 5$) exceed the experimental values.

Figure 7 shows the current-voltage characteristic of a Josephson structure with a single bicrystal boundary at $T=4.2$ K and the corresponding detector response $\eta(V)$ to microwave radiation with a frequency $f_e=30.5$ GHz for two values of the constant magnetic field $B=52$ and $-153 \mu\text{T}$. This figure also presents the results of the numerical simulation for an array with $N=5$ and magnetic flux Φ/Φ_0 corresponding to the experimental values of $I_c(B)$. We note that the form, similar to odd-symmetric resonance, of both the experimental and theoretical plots of $\eta(V)$ attests to the syn-

chronous detection process known for a Josephson junction conforming to the RSJ model. At the same time, subharmonic responses are clearly visible at $V=V_{1/2,1}$ in both the theoretical plots and the experimental plot for a magnetic field corresponding to values of I_c which are depressed considerably in comparison with the maximum value. The difference between experiment and calculation is probably due to the difference between the experimental dependence of $R_d(V)$ and the theoretical dependence and by the influence of excess noise, which broadens the Josephson emission line.^{7,12} When $I_c = I_c^{\max}(B)$ the subharmonic response is not observed experimentally, and in the calculations it has a less pronounced character and is asymmetric relative to $\eta=0$, pointing out that the processes are not coherent under these conditions.

The simulation of a bicrystal boundary by a parallel array of Josephson junctions also accounts for some other experimentally observed features. For example, in the plots of $i_{c1}(i_{RF})$ for $f_e=44$ GHz and 52 GHz we observed an N -shaped feature at $i_{RF}\approx 0.1$ (see Fig. 3) corresponding in both cases to the first maximum in the plot of the subharmonic step $i_{1/2}(i_{RF})$, which had a height $i_{1/2}^{\max}=0.4$ when $f_e=52$ GHz. An N -shaped feature was also noted in the plot of $i_c(i_{RF})$ in Ref. 10, in which a single YBCO grain boundary was modeled by two Josephson junctions conforming to the RSJ model and connected in parallel. Oscillating plots of the Josephson current steps with $n=1/2, 1, 3/2,$ and 2 in a magnetic field corresponding to the minima of the experimental plot of $I_c(B)$ were also obtained on the basis of this model in Ref. 10, and the maximum height of the subharmonic current step had a value $i_{1/2}^{\max}\approx 0.2$, which is 3.5 times smaller than the value in our experimental case (see the insert in Fig. 4). The experimentally observed higher value of $i_{c1}>1$ (see Fig. 3) at weak microwave fields ($i_{RF}<0.1$) is attributable to the slow variation of the external magnetic field, which is significant for systems with Josephson junctions connected in parallel even when ordinary shielding with low residual magnetization is employed.

5. CONCLUSIONS

The results presented here of an experimental investigation of a high- T_c superconducting thin-film bridge spanning a step on a substrate without a break in the film are typical of Josephson structures formed on grain boundaries. One special feature of such Josephson structures is the significant nonuniformity of the distribution of the critical current density over the broad temperature range $T<T_c$, which results in considerable deviation of their behavior from the RSJ model. At the same time, the investigation of the dynamics of the transformation of the current-voltage characteristic under the action of a microwave field revealed that the critical frequency of such Josephson junctions is close to the approximate value $f_c\approx V_0/\Phi_0$ following from the RSJ model. The experimentally observed deviations from the RSJ model [the "SQUID-like" dependence of $I_c(B)$, the presence of subharmonic steps on the perturbed current-voltage characteristics at a nonzero magnetic field close to the earth's field, etc.] are at least qualitatively explained by the model of a

bicrystal boundary in the form of a parallel array of several inductively coupled Josephson junctions described by the RSJ model.

The observation of a detector response at certain values of the magnetic field to a weak microwave signal which does not perturb the current-voltage characteristic of a single bicrystal boundary at voltages corresponding to the $n=1/2$ subharmonic attests to a significant deviation of the phase-frequency characteristics of the spontaneous emission spectrum of the bicrystal boundary (according to the model of an array of Josephson junctions connected in parallel) from the spectrum of a single Josephson junction conforming to the RSJ model. This means that the current-voltage characteristic and the spectrum of the spontaneous electromagnetic emission of a single bicrystal boundary are strongly dependent on a weak external magnetic field $B\ll\Phi_0 wd$, which, in the final analysis, determines its high-frequency dynamics under microwave electromagnetic radiation. The experimental investigation of two bicrystal boundaries connected in series showed that an interaction between them is observed only when there is a strong ($i_{RF}>1$) synchronizing microwave field. The broad range of variation of f_e and P_e corresponding to frequency locking of the double bicrystal boundary that was detected attests to a nonresonant interaction between them. The experimental lack of phase locking of the double bicrystal boundary when $i_{RF}\ll 1$, even in the case in which their critical currents were equalized by the magnetic field, attests to the small value of the coupling energies between the bicrystal boundaries.

We thank T. Claeson, J. Myugind, and N. Pedersen for discussing the results obtained, and G. Fischer for helping to perform the experiments. This research was partially supported by the Scientific Council for High- T_c Superconductivity Program, the INTAS Project of the European Community, and the International HTSC Project.

*Moscow State University, Moscow, Russia

[†]Chalmers University of Technology, Göteborg, Sweden

¹K. K. Likharev and B. T. Ul'rikh, *Systems with Josephson Junctions* [in Russian], MGU, Moscow (1978), p. 446.

²D. Dimos, P. Chaudhari, and J. Mannhart, *Phys. Rev. B* **41**, 4038 (1990).

³J. Halbritter, *Phys. Rev. B* **48**, 9735 (1993).

⁴B. H. Moeckly, D. K. Lathrop, and R. A. Buhrman, *Phys. Rev. B* **47**, 400 (1993).

⁵C. L. Jia, B. Kabius, K. Urban *et al.*, *Physica C* **196**, 211 (1992).

⁶E. Samelli, P. Chaudhari, and J. Lacey, *Appl. Phys. Lett.* **62**, 777 (1993).

⁷Yu. Ya. Divin, A. V. Andreev, G. M. Fischer *et al.*, *Appl. Phys. Lett.* **62**, 1295 (1993).

⁸J. Ramos, Z. G. Ivanov, E. Olsson, S. Zarembinski, and T. Claeson, *Appl. Phys. Lett.* **63**, 2141 (1993).

⁹J. A. Edwards, J. S. Satchell, N. G. Chew *et al.*, *Appl. Phys. Lett.* **60**, 2433 (1992).

¹⁰E. A. Early, R. L. Steiner, A. F. Clark, and K. Char, *Phys. Rev. B* **50**, 9409 (1994).

¹¹R. L. Kautz, S. P. Benz, and C. D. Reintsema, *Appl. Phys. Lett.* **65**, 1445 (1994).

¹²G. A. Ovsyannikov, J. Ramos, and Z. G. Ivanov, *Pis'ma Zh. Tekh. Fiz.* **20**, 31 (1994) [*Tech. Phys. Lett.* **20**, 354 (1994)].

- ¹³L. É. Amatuni, R. M. Martirosyan, and K. I. Konstantinyan, *Pis'ma Zh. Tekh. Fiz.* **20**, 86 (1994) [*Tech. Phys. Lett.* **20**, 128 (1994)].
- ¹⁴G. A. Ovsyannikov, G. E. Babayan, V. N. Laptev, and V. I. Makhov, *IEEE Trans. Magn.* **MAG-27**, 2688 (1991).
- ¹⁵S. V. Polonsky, V. K. Semenov, and P. N. Shevchenko, in *Third International Superconducting Electronics Conference, Extended Abstracts*, University of Strathclyde, Glasgow (1991), p. 160.
- ¹⁶L. É. Amatuni, V. N. Gubankov, and G. A. Ovsyannikov, *Fiz. Nizk. Temp.* **9**, 939 (1983) [*Sov. J. Low Temp. Phys.* **9**, 484 (1983)].
- ¹⁷M. Octavio and W. J. Skocpol, *J. Appl. Phys.* **50**, 3505 (1979).
- ¹⁸S. I. Borovitskiĭ and A. M. Klushin, *Pis'ma Zh. Tekh. Fiz.* **7**, 890 (1981) [*Sov. Tech. Phys. Lett.* **7**, 382 (1981)].

Translated by P. Shelnitz